

Single and double inclusive particle production in d+Au collisions at RHIC, leading twist and beyond

Javier L. Albacete

Institut de Physique Théorique, CEA/Saclay, 91191 Gif-sur-Yvette cedex, France

Cyrille Marquet

Physics Department, Theory Unit, CERN, 1211 Genève 23, Switzerland

Abstract

We discuss the evidence for the presence of QCD saturation effects in the data collected in d+Au collisions at RHIC. In particular we focus our analysis on forward hadron yields and azimuthal correlations. Approaches alternative to the CGC description of these two observables are discussed in parallel.

Keywords: Relativistic Heavy Ion Collisions, Color Glass Condensate

1. Introduction

The large amount of experimental data collected at RHIC during the last decade over a wide kinematical range allows to explore novel QCD effects. Indeed RHIC measurements present a number of features which are well described within the Color Glass Condensate effective theory of QCD at high energies (see e.g. [1, 2] and references therein). The main physical ingredient in the CGC is the inclusion of unitarity effects through the proper consideration of both non-linear recombination effects in the quantum evolution of hadronic wave functions and multiple scatterings at the level of particle production. Such effects are expected to be relevant when partons with a small enough energy fraction x are probed in the nuclear (or, in full generality, hadronic) wave function.

Email addresses: javier.lopez-albacete@cea.fr (Javier L. Albacete),
cyrille.marquet@cern.ch (Cyrille Marquet)

The CGC formalism itself is only reliable at small x , in that kinematic regime gluon densities are large and gluon self-interactions become highly probable, thus taming, or saturating, further growth of the gluon occupation numbers. While the need for unitarity effects comprised in the CGC is, at a theoretical level, clear, the real challenge from a phenomenological point of view is to assess to what extent they are present in available data. Such is a difficult task, since different physical mechanisms concur in data, and also because the limit of asymptotically high energy in which the CGC formalism is developed may not be realized in current experiments.

Notwithstanding these difficulties, we argue below that RHIC data [3, 4, 5] offer compelling evidence for the presence of saturation effects. Such claim is based on the successful simultaneous description of the suppression of particle production [6] and azimuthal correlations [7] at forward rapidities in d+Au collisions compared to p+p collisions, using the most up-to-date theoretical tools available in the CGC approach. We focus on forward particle production for the following reason: such processes are sensitive only to high-momentum partons inside one of the colliding hadron, which appears dilute, while mainly small-momentum partons inside the other dense hadron contribute to the scattering. Since the high- x part of a proton wave function is well understood in perturbative QCD, forward particle production in high-energy d+Au (or generically p+A) collisions is ideal to investigate the small- x part of the nucleus wave function.

In the case of single-inclusive hadron production $pA \rightarrow hX$, denoting p_\perp and y the transverse momentum and rapidity of the final state particles, the partons that can contribute to the cross section have a fraction of longitudinal momentum bounded from below, by x_p (for partons from the proton wave function) and x_A (for partons from the nucleus wave function) given by

$$x_p = x_F, \quad x_A = x_F e^{-2y}, \quad (1)$$

where we introduced the Feynman variable $x_F = |p_\perp| e^y / \sqrt{s_{NN}}$ with $\sqrt{s_{NN}}$ the collision energy per nucleon. With $\sqrt{s_{NN}} \gg |p_\perp|$ and forward rapidities $y > 0$, the process features $x_p \lesssim 1$ and $x_A \ll 1$, meaning that the scattering involves on the proton side, quantum fluctuations well understood in QCD, and on the nucleus side, quantum fluctuations whose non-linear QCD dynamics can be studied.

In the case of double-inclusive hadron production $pA \rightarrow h_1 h_2 X$, denoting $p_{1\perp}$, $p_{2\perp}$ and y_1 , y_2 the transverse momenta and rapidities of the final-state

particles, the Feynman variables are $x_i = |p_{i\perp}|e^{y_i}/\sqrt{s_{NN}}$ and x_p and x_A read

$$x_p = x_1 + x_2, \quad x_A = x_1 e^{-2y_1} + x_2 e^{-2y_2}. \quad (2)$$

Therefore, only the forward-forward case is sensitive to values of x as small as in the single particle production case: $x_p \lesssim 1$ and $x_A \ll 1$. The central-forward measurement does not probe such kinematics: moving one particle forward increases significantly the value of x_p compared to the central-central case (for which $x_p = x_A = |p_\perp|/\sqrt{s_{NN}}$), but decreases x_A only marginally. For this reason we shall refer to these two situations as mid-rapidity ones. The approximations made in CGC calculations apply best with forward-rapidity observables, at RHIC mid-rapidity ones are contaminated too much by large- x physics to be treated at a quantitative level.

Saturation-based approaches were the only ones to correctly predict the suppression of forward particle production [8, 9] and the azimuthal decorrelation of forward hadron pairs [10]. In the following, we also comment on alternative mechanisms that successfully describe mid-rapidity particle production in d+Au collisions. We note that, while some of these approaches are also able to describe, a posteriori, the suppression of forward yields, we are not aware of any formalism that can also describe the azimuthal decorrelation of forward hadron pairs.

2. Nuclear modifications at mid-rapidity

In relativistic heavy-ion collisions, nuclear effects on single particle production are typically evaluated in terms of ratios of particle yields called nuclear modification factors:

$$R_{pA}^h = \frac{dN^{pA \rightarrow hX}/dyd^2p_\perp}{N_{coll} dN^{pp \rightarrow hX}/dyd^2p_\perp}, \quad (3)$$

where N_{coll} is the number of nucleon-nucleon collisions in the p+A collision. If high-energy nuclear reactions were a mere incoherent superposition of nucleon-nucleon collisions, then the observed R_{pA} would be equal to unity. However, RHIC measurements in d+Au collisions (or peripheral Au+Au collisions) [3, 4] exhibit two opposite regimes: at mid rapidities the nuclear modification factors exhibit an enhancement in particle production at intermediate momenta $|p_\perp| \sim 2 \div 4$ GeV. In turn, a suppression at smaller momenta is observed. However, at forward rapidities the Cronin enhancement disappears, turning into an almost homogeneous suppression.

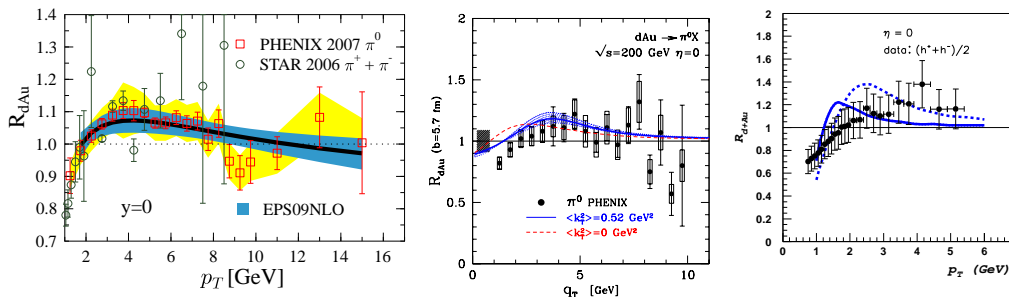


Figure 1: RHIC experimental results for $R_{dAu}^{\pi^0}$ at $\eta = 0$ compared with different calculations. From left to right: comparison with EPS09 parametrization [11], a Glauber-Eikonal calculation [12], and the CGC approach of [13].

Single-hadron production data at mid-rapidity have been successfully analyzed through different formalisms and techniques. Below we sketch an incomplete, but representative list of the variety in the theory spectrum:

- **Leading-twist perturbation theory.** The assumption is that standard collinear factorization holds in nuclear reactions, meaning that highly-virtual partons in nuclei behave independently as they do in protons. For each parton species i the nuclear parton distribution functions are taken to be proportional to that of a proton: $f_i^A(x, Q^2) = R_i^A(x, Q^2) f_i^N(x, Q^2)$. The proportionality factors $R_i^A(x, Q^2)$ are fitted, in part, to available d+Au data and in some cases, as in the EPS parametrization [11], evolved according to DGLAP evolution. The resulting data description is displayed in Fig. 1a.
- **Glauber-eikonal multiple scatterings.** This approach takes into account power corrections to the leading-twist approximation. It relies on a resummation of incoherent multiple scatterings. Typically, this results in a momentum broadening of the scattered parton which is responsible for the Cronin enhancement and, due to unitarity constraints, to a depletion of particle production at small transverse momenta, in agreement with the qualitative features of the data as can be seen in Fig. 1b. Performing the complete resummation including energy-momentum conservation is a challenging task. Sometimes, a detour of the strict calculation is taken by resorting to unintegrated parton distributions which include information about the intrinsic trans-

verse momentum of the partons k_0 , and the average transverse momentum gained during the interaction with the nucleus Δk : $f_i^A(x, Q^2) \rightarrow F_i^A(x, Q^2, \langle k_0^2 \rangle + \langle \Delta k^2 \rangle (\sqrt{s}, b, p_\perp)$. While the intrinsic k_0 is adjusted in p+p collisions, the gained transverse momentum is let to depend on the collision energy, centrality and p_\perp of the detected hadron.

- **Color Glass Condensate.** The CGC approach resums all power corrections which are dominant in the high-energy/small- x limit. It relies on two main assumptions: the scattering process is fully coherent and the propagation of the leading parton through the nucleus is eikonal, i.e. the momentum transferred during the collision is only transverse. Then, non-linearities or saturation effects can be taken into account either at the semiclassical level or, more accurately, including the quantum corrections embodied in the JIMWLK evolution equation. The work presented in Fig. 1c relies on a combination of both, with quantum corrections modeled according to analytical estimates [13]. Note that in the CGC framework, the saturation scale Q_s which characterizes the onset of non-linear effects in the nuclear wave function, also determines both the intrinsic transverse momentum and the amount of it gained during the collision. In the small- x limit, it is not possible to distinguish saturation from multiple scatterings, such a separation would be frame dependent. Both become important when a large gluon density is reached, and including one without the other is not consistent.

Simply by looking at Fig. 1, one concludes that the three different approaches above offer a comparably good description of the data, so it is difficult to extract any clean conclusion about the physical origin of the Cronin enhancement. This is probably due to the kinematic region probed in these measurements. For a hadron momentum of $|p_\perp| \sim 2$ GeV, one is sensitive to $(x_p \sim) x_A \sim 0.01 \div 0.1$. In this region different physical mechanisms concur, so neither of the physical assumptions underlying the approaches above is completely fulfilled. Indeed, the coherence length, estimated to be $l_c \sim 1/(2m_N x_A) \sim 1 \div 10$ fm is, on average, smaller than the nuclear length, so the fully coherent treatment of the collision implicit in the CGC is not completely justified, and large- x corrections are expected to be relevant. Moreover, both the coherent or incoherent treatments of the collision in [12, 13] need to invoke the presence of an intrinsic scale, presumably of non-perturbative origin, of the order of 1 Gev in order to reproduce the data, whose dynamical origin is not evident at all.

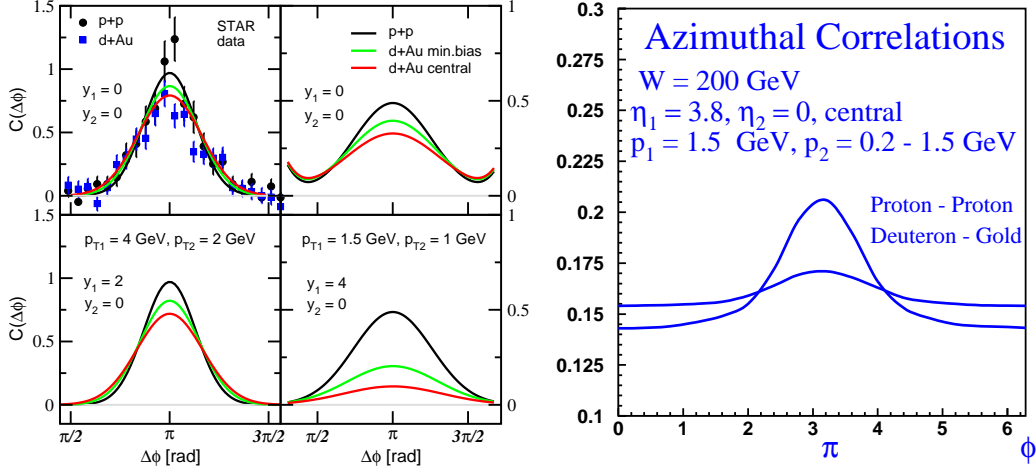


Figure 2: The coincidence probability at mid-rapidity as a function of $\Delta\phi$. RHIC data show that in the central-central case the away-side peak is similar in d+Au and p+p collisions. In the central-forward case, the Glauber-eikonal (left plot from [14]) and CGC (right plot from [15]) calculations predict that the away-side peak is suppressed in d+Au compared to p+p collisions, in agreement with later data.

More insight is gained with di-hadron correlations. In particular, let us focus on the $\Delta\phi$ dependence of the double-inclusive hadron spectrum, where $\Delta\phi$ is the difference between the azimuthal angles of the measured particles h_1 and h_2 . Nuclear effects on di-hadron correlations are typically evaluated in terms of the coincidence probability to, given a trigger particle in a certain momentum range, produce an associated particle in another momentum range. In a p+p or p+A collision, the coincidence probability is given by $CP(\Delta\phi) = N_{pair}(\Delta\phi)/N_{trig}$ with

$$N_{pair}(\Delta\phi) = \int_{y_i, |p_{i\perp}|} \frac{dN^{pA \rightarrow h_1 h_2 X}}{d^3 p_1 d^3 p_2}, \quad N_{trig} = \int_{y, p_\perp} \frac{dN^{pA \rightarrow h X}}{d^3 p}. \quad (4)$$

First measurements were performed at RHIC at mid-rapidity by the PHENIX and STAR collaborations [4, 16]. In the central-central case, the coincidence probability features a near-side peak around $\Delta\phi = 0$, when both measured particles belong to the same mini-jet, and an away-side peak around $\Delta\phi = \pi$, corresponding to hadrons produced back-to-back. In the central-forward case, there is naturally no near-side peak.

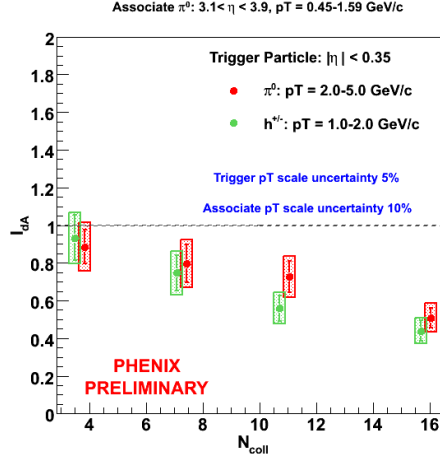


Figure 3: Central-forward preliminary I_{dAu} data as a function of centrality [17]. In central collisions, the integral of the coincidence probability is about half that in p+p collisions, reflecting the depletion of the away-side peak. Collinear factorization cannot reproduce this behavior, while both Glauber-eikonal and CGC calculations predicted it.

Either in p+p or d+Au collisions, the sizeable width of the away-side peak cannot be described within the leading-twist collinear factorization framework. This indicates that, while it may not be obvious in single particle production, power corrections are important when $|p_{\perp}| \sim 2$ GeV. At such low transverse momenta, collinear factorization does not provide a global picture of particle production at RHIC, even at mid-rapidity. On the contrary, both the Glauber multiple scattering [14] and CGC [15] approaches can qualitatively describe the data, including the depletion of the away-side peak in d+Au collisions when going from central-central to central-forward production. This is illustrated in Fig. 2. Such a depletion does not occur in p+p collisions, it is due to nuclear-enhanced power corrections, and therefore the p+A to p+p ratio of the integrated coincidence probabilities

$$I_{pA} = \frac{\int d\phi CP_{pA}(\Delta\phi)}{\int d\phi CP_{pp}(\Delta\phi)} \quad (5)$$

is below unity. In Fig. 3, recent PHENIX data on I_{dAu} are displayed as a function of centrality. At the moment, since x_A is not that small, it is not clear whether the mechanism for this suppression is due to saturation effects rather than incoherent multiple scatterings.

3. Moving forward

As outlined in the introduction, data collected in the deuteron fragmentation region offer a cleaner opportunity to explore saturation effects. Let us first explain our implementation of the CGC framework. The CGC is equipped with a set of non-linear renormalization group equations to describe the evolution of hadronic wave functions towards small- x . In the large- N_c limit, they reduce to the BK equation [18, 19]. The recent determination of running coupling corrections to the original leading-log equations [20, 21] has proven an essential step in promoting the BK equation to a phenomenological tool. Indeed, the running coupling BK equation (rcBK) has been employed to successfully describe inclusive structure functions in e+p scattering [22] and also the energy and multiplicity dependence of total hadron multiplicities in Au+Au collisions at RHIC [23].

The rcBK equation reads

$$\frac{\mathcal{N}(r, Y)}{\partial \ln(1/x)} = \int d^2\mathbf{r}_1 K^{\text{run}}(\mathbf{r}, \mathbf{r}_1, \mathbf{r}_2) [\mathcal{N}(r_1, Y) + \mathcal{N}(r_2, Y) - \mathcal{N}(r, Y) - \mathcal{N}(r_1, Y)\mathcal{N}(r_2, Y)] , \quad (6)$$

where $\mathbf{r}_2 = \mathbf{r} - \mathbf{r}_1$ (we use the notation $v \equiv |\mathbf{v}|$ for two-dimensional vectors in Eq. (6) and Eq. (7)). $\mathcal{N}(r, Y)$ is the dipole scattering amplitude in the fundamental representation, with $Y = \ln(x_0/x)$ the rapidity and r the dipole transverse size. It turns out that the evolution kernel

$$K^{\text{run}}(\mathbf{r}, \mathbf{r}_1, \mathbf{r}_2) = \frac{N_c \alpha_s(r^2)}{2\pi^2} \left[\frac{1}{r_1^2} \left(\frac{\alpha_s(r_1^2)}{\alpha_s(r_2^2)} - 1 \right) + \frac{r^2}{r_1^2 r_2^2} + \frac{1}{r_2^2} \left(\frac{\alpha_s(r_2^2)}{\alpha_s(r_1^2)} - 1 \right) \right] \quad (7)$$

proposed in [20] minimizes the role of higher order corrections, making it better suited for phenomenological applications. Detailed discussions about other prescriptions proposed to define the running coupling kernel, and about the numerical method to solve the rcBK equation can be found in [24].

Eq. (6) needs to be supplemented with initial conditions, which we choose to be of the McLerran-Venugopalan type:

$$\mathcal{N}(r, Y=0) = 1 - \exp \left[-\frac{r^2 \bar{Q}_{s0}^2}{4} \ln \left(\frac{1}{\Lambda r} + e \right) \right] , \quad (8)$$

where $\Lambda = 0.241$ GeV. This introduces two free parameters: the value x_0 where the evolution starts and the initial saturation scale felt by quarks \bar{Q}_{s0} .

3.1. Nuclear modification factors

According to Ref. [25], the differential cross section for forward hadron production in p+A collisions is given by

$$\frac{dN^{pA \rightarrow hX}}{dy d^2p_\perp} = K \sum_q \int_{x_F}^1 \frac{dz}{z^2} \left[x_1 f_{q/p}(\tilde{x}_p, p_\perp^2) F\left(\tilde{x}_A, \frac{p_\perp}{z}\right) D_{h/q}(z, p_\perp^2) + x_1 f_{g/p}(\tilde{x}_p, p_\perp^2) \tilde{F}\left(\tilde{x}_A, \frac{p_\perp}{z}\right) D_{h/g}(z, p_\perp^2) \right], \quad (9)$$

where the unintegrated gluon distributions F and \tilde{F} are related to the dipole scattering amplitude through Fourier transformations:

$$F(x, k) = \int \frac{d^2\mathbf{r}}{(2\pi)^2} e^{-i\mathbf{k}\cdot\mathbf{r}} [1 - \mathcal{N}(r, Y = \ln(x_0/x))] , \quad (10)$$

$$\tilde{F}(x, k) = \int \frac{d^2\mathbf{r}}{(2\pi)^2} e^{-i\mathbf{k}\cdot\mathbf{r}} [1 - \mathcal{N}(r, Y = \ln(x_0/x))]^2 . \quad (11)$$

In principle \tilde{F} is the Fourier transform of the dipole scattering amplitude in the adjoint representation [26, 27, 28], we have used to large- N_c limit in Eq. (11). In Eq. (9), $f_{i/p}$ and $D_{h/i}$ refer to the parton distribution function (pdf) of the incoming proton and to the final-state hadron fragmentation function respectively. Here we will use the CTEQ6 NLO pdf's [29] and the DSS NLO fragmentation functions [30, 31]. We have assumed that the factorization and fragmentation scales are both equal to the transverse momentum of the produced hadron. Note that the projectile in our calculations is actually a deuteron, and we obtain the neutron pdf from the proton one assuming isospin symmetry.

For light hadron production discussed here, the difference between the rapidity and pseudo-rapidity η of the produced hadron can be neglected, yielding the following kinematics: $\tilde{x}_p = x_F/z$ and $\tilde{x}_A = (x_F/z) \exp(-2y)$ with $x_F = \sqrt{m_h^2 + p_\perp^2}/\sqrt{s_{NN}} \exp(\eta) \approx |p_\perp|/\sqrt{s_{NN}} \exp(y)$ introduced before. Due to parton fragmentation, the values of \tilde{x} 's actually probed are generically higher than x_p and x_A defined in Eq. (1).

With this set up we reach a very good description [6] of the forward negatively charged hadron and neutral pion yields measured by the BRAHMS [3] and STAR [4] collaborations respectively, in p+p and minimum bias d+Au collisions. The parameters of the fit are $x_0 = 0.025 \div 0.005$ (0.0075) and $\bar{Q}_{s0}^2 = 0.5 \div 0.4$ (0.2) GeV² for the initial nucleus (proton) wave function.

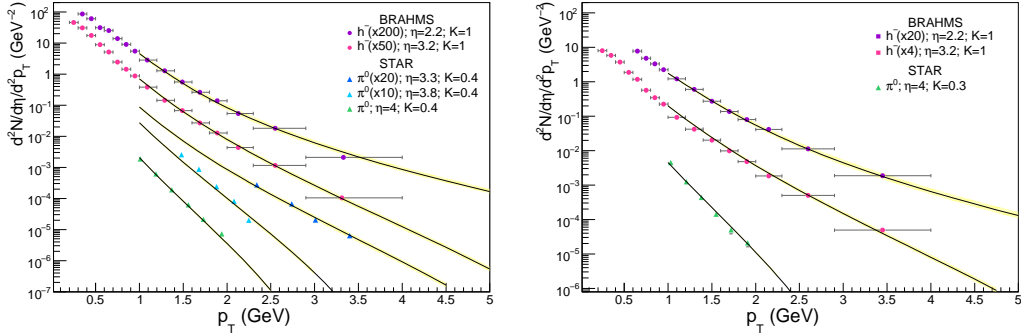


Figure 4: Negatively charged hadrons and neutral pions at forward rapidities at RHIC in p+p (left) and minimum bias d+Au (right) collisions, compared to our calculation [6].

Moreover, no K -factors are needed except for the most forward pions $\eta > 3$, where we find that $K = 0.3$ (0.4) is needed to describe the data.

Our results are shown in Fig. 4. By simply taking the ratios of the corresponding spectra, we get a very good description of the nuclear modification factors at forward rapidities, and this is shown in Fig. 5a. It should be noted that we use the same normalization as experimentalists do in their analysis of minimum bias d+Au collisions: $N_{coll} = 7.2$. Physically, the observed suppression is due to the relative enhancement of non-linear terms in the small- x evolution of the nuclear wave function with respect to that of a proton.

After the data confirmed the CGC expectations, it has been argued that the observed suppression of particle production at forward rapidities is not an effect associated to the small values of x_A probed in the nuclear wave function, but rather to energy-momentum conservation corrections relevant for $x_F \rightarrow 1$ [32, 33]. Such corrections are not present in the CGC, built upon the eikonal approximation (this may explain why a K -factor is needed to describe the suppression of very forward pions). The energy degradation of the projectile parton, neglected in the CGC, through either elastic scattering or induced gluon brehmstrahlung would be larger in a nucleus than in proton on account of the stronger color fields of the former, resulting in the relative suppression observed in data. A successful description of forward ratios based on the energy loss calculation in [32] is shown in Fig. 5b. Calculating forward di-hadron correlations in both frameworks could help pin down which is the correct picture. In the following, we show that the CGC calculations predicts correctly the azimuthal distribution.

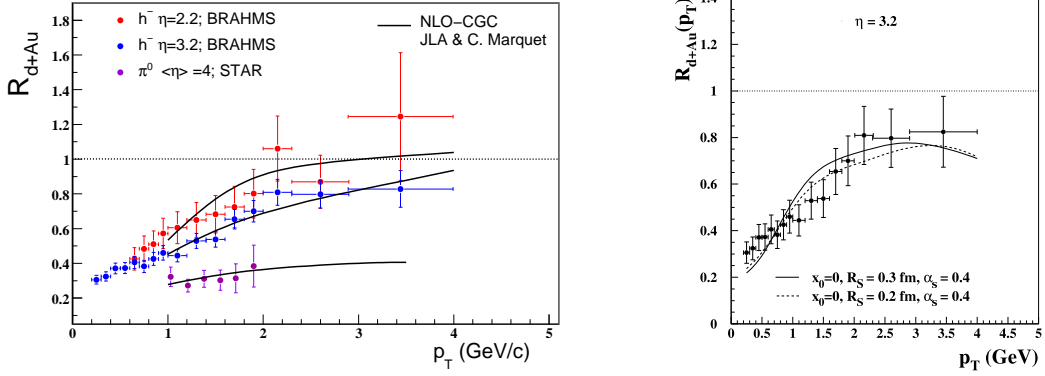


Figure 5: Nuclear modification factors at forward rapidities in minimum bias d+Au collisions in CGC [6] (left) and energy-loss [32] (right) calculations.

3.2. Di-hadron azimuthal correlations

The kinematic range for forward particle detection at RHIC is such that $x_p \sim 0.4$ and $x_A \sim 10^{-3}$. Therefore the dominant partonic subprocess is initiated by valence quarks in the proton and, at lowest order in α_s , the $pA \rightarrow h_1 h_2 X$ double-inclusive cross-section is obtained from the $qA \rightarrow qgX$ cross-section, the valence quark density in the proton $f_{q/p}$, and the appropriate hadron fragmentation functions $D_{h/q}$ and $D_{h/g}$:

$$\begin{aligned}
 dN^{pA \rightarrow h_1 h_2 X} &= \int_{x_1}^1 dz_1 \int_{x_2}^1 dz_2 \int_{\frac{x_1+x_2}{z_1+z_2}}^1 dx f_{q/p}(x, \mu^2) \\
 &\times \left[dN^{qA \rightarrow qgX} \left(xP, \frac{p_1}{z_1}, \frac{p_2}{z_2} \right) D_{h_1/q}(z_1, \mu^2) D_{h_2/g}(z_2, \mu^2) + \right. \\
 &\left. dN^{qA \rightarrow qgX} \left(xP, \frac{p_2}{z_2}, \frac{p_1}{z_1} \right) D_{h_1/g}(z_1, \mu^2) D_{h_2/q}(z_2, \mu^2) \right]. \quad (12)
 \end{aligned}$$

We shall use CTEQ6 NLO quark distributions [29] and KKP NLO fragmentation functions [34]. The factorization and fragmentation scales are both chosen equal to the transverse momentum of the leading hadron, which we choose to denote hadron 1, $\mu = |p_{1\perp}|$. We have assumed independent fragmentation of the two final-state hadrons, therefore Eq. (12) cannot be used to compute the near-side peak around $\Delta\Phi = 0$. Doing so would require the use of poorly-known di-hadron fragmentation functions, rather we will focus on the away-side peak around $\Delta\Phi = \pi$ where saturation effects are important.

For the proton, one has $x_p < x < 1$, and if x_p would be smaller (this will be the case at the LHC), the gluon initiated processes $gA \rightarrow q\bar{q}X$ and $gA \rightarrow ggX$ should also be included in Eq. (12). For the nucleus, we shall see that the parton momentum fraction varies between x_A and $e^{-2y_1} + e^{-2y_2}$. Therefore with large enough rapidities, only the small- x part of the nuclear wave function is relevant when calculating the $qA \rightarrow qqX$ cross section, and that cross section cannot be factorized further: $dN^{qA \rightarrow qqX} \neq f_{g/A} \otimes dN^{qg \rightarrow qqX}$. Indeed, when probing the saturation regime, $dN^{qA \rightarrow qqX}$ is expected to be a non-linear function of the nuclear gluon distribution, which is itself, through evolution, a non-linear function of the gluon distribution at higher x .

Using the CGC approach to describe the small- x part of the nucleus wave function, the $qA \rightarrow qqX$ cross section was calculated in [35, 36, 37, 10]. It was found that the nucleus cannot be described by only the single-gluon distribution, a direct consequence of the fact that small- x gluons in the nuclear wave function behave coherently, and not individually. The $qA \rightarrow qqX$ cross section is instead expressed in terms of correlators of Wilson lines (which account for multiple scatterings), with up to a six-point correlator averaged over the CGC wave function. At the moment, it is not known how to practically evaluate the six-point function. In the large- N_c limit, it factorizes into a dipole scattering amplitude times a trace of four Wilson lines, and the latter can in principle be obtained by solving an evolution equation written down in [35]. However, this implies a significant amount of numerical work and also requires to introduce an unknown initial condition.

Rather we shall follow the approach of [10], and use an approximation that allows to express the six-point function in terms of the two-point function Eq. (10). The resulting cross section for the inclusive production of the quark-gluon system in the scattering of a quark with momentum xP^+ off the nucleus A reads [10]:

$$\begin{aligned} \frac{dN^{qA \rightarrow qqX}}{d^3k d^3q} &= \frac{\alpha_S C_F}{4\pi^2} \delta(xP^+ - k^+ - q^+) F(\tilde{x}_A, \Delta) \\ &\times \sum_{\lambda\alpha\beta} |I_{\alpha\beta}^\lambda(z, k_\perp - \Delta; \tilde{x}_A) - \psi_{\alpha\beta}^\lambda(z, k_\perp - z\Delta)|^2, \quad (13) \end{aligned}$$

where q and k are the momenta the quark and gluon respectively, and with $\Delta = k_\perp + q_\perp$ and $z = k^+/xP^+$. In this formula, \tilde{x}_A denotes the longitudinal momentum fraction of the gluon in the nucleus, and $\tilde{x}_A = x_1 e^{-2y_1}/z_1 + x_2 e^{-2y_2}/z_2 > x_A$ when the cross section Eq. (13) is plugged into Eq. (12).

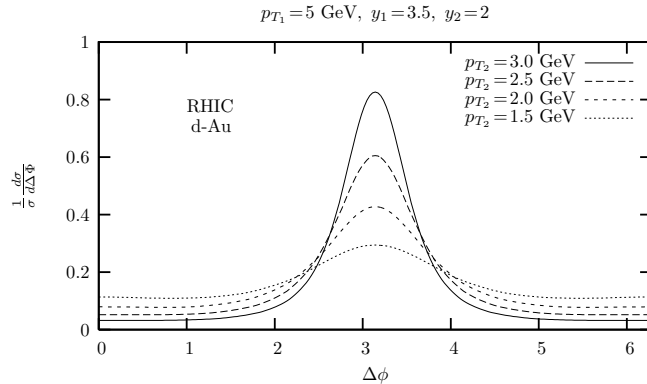


Figure 6: The $\Delta\phi$ distribution $(1/\sigma)d\sigma/d\Delta\phi$ computed in [10] at fixed $y_1 = 3.5$, $y_2 = 2$ and $|p_{1\perp}| = 5$ GeV. The azimuthal correlation is suppressed as $|p_{2\perp}|$ decreases, this is due to the onset of non-linearities in the nuclear wave function.

The second line of Eq. (13) features a k_T -factorization breaking term:

$$I_{\alpha\beta}^\lambda(z, k_\perp; x) = \int d^2q_\perp \psi_{\alpha\beta}^\lambda(z, q_\perp) F(x, k_\perp - q_\perp), \quad (14)$$

and where $\psi_{\alpha\beta}^\lambda$ is the well-known amplitude for $q \rightarrow qg$ splitting (λ , α and β are polarization and helicity indices). While no additional information than the two-point function is needed to compute Eq. (13), since higher-point correlators needed in principle have been expressed in terms of $F(x, k_\perp)$, the cross section is still a non-linear function of that gluon distribution, invalidating k_T -factorization. The rather simple form of the k_T -factorization breaking term is due to the use of a Gaussian CGC color source distribution, and to the large- N_c limit. Finally, the factor $\delta(xP^+ - k^+ - q^+)$ in Eq. (13) is due to the fact that the eikonal approximation, valid at high energies, is used to compute the $qA \rightarrow qgX$ cross section. The delta function is a manifestation of the fact that in a high-energy hadronic collision, the momentum transfer is mainly transverse.

Before comparing our predictions to the recent RHIC data, we first display in Fig. 6 the predictions for the $\Delta\phi$ distributions made in [10] when only the leading-order BK evolution was known. The different curves are obtained for fixed y_1 , y_2 and $|p_{1\perp}|$, while $|p_{2\perp}|$ is varied. Although these results are only qualitative since for instance parton fragmentation was not included, the suppression of the $\Delta\phi$ distribution as $|p_{2\perp}|$ gets closer to the saturation scale was predicted.

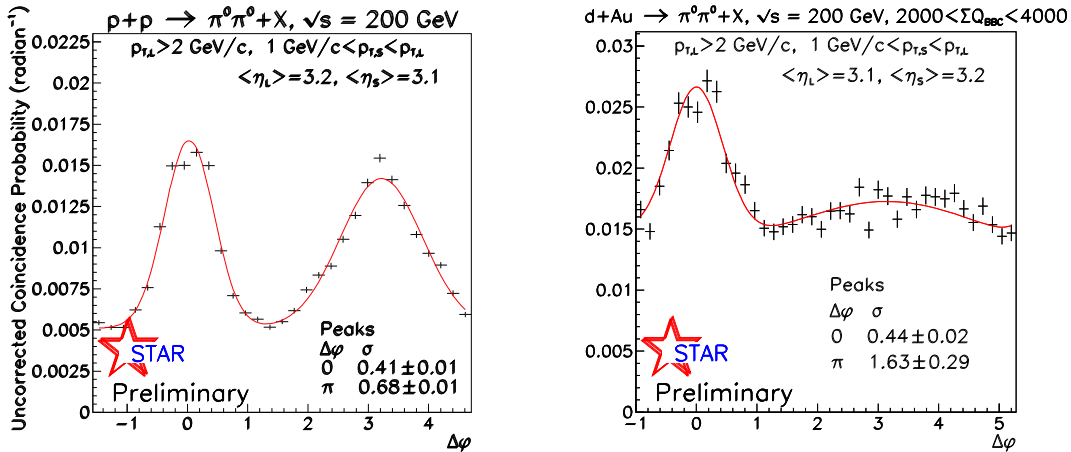


Figure 7: The coincidence probability as a function of $\Delta\phi$ for p+p (left) and central d+Au (right) collisions. These preliminary data from [5] show a striking nuclear modification of di-hadron azimuthal correlations. The away-side peak, corresponding to hadrons emitted back-to-back, is prominent in p+p collisions but is absent in the central d+Au case. Such production of monojets was anticipated in the CGC as a signal of parton saturation.

Then, the derivation of the rcBK equation made robust quantitative calculations possible. Indeed, after the parameters of the theory (x_0 and \bar{Q}_{s0} for both the proton and the gold nucleus) were constrained by single-inclusive forward spectra, parameter-free predictions for the coincidence probability $CP(\Delta\phi)$ could be made [7]. In Eq. (4), when computing N_{pair} from Eq. (12) and N_{trig} from Eq. (9) for d+Au and p+p collisions, the integration bounds for the rapidities are $2.4 < y < 4$, in order to compare with RHIC data [5]. In addition, such a restriction does insure that only small-momentum partons are relevant in the nucleus wave function, as is assumed in our calculation. For the trigger (leading) particle $|p_{1\perp}| > 2 \text{ GeV}$ and for the associated (sub-leading) hadron $1 \text{ GeV} < |p_{2\perp}| < |p_{1\perp}|$.

The recent data obtained by the STAR collaboration for the coincidence probability obtained with two neutral pions are displayed in Fig. 7 for both p+p and central d+Au collisions. The nuclear modification of the di-pion azimuthal correlation is quite impressive, the prominent away-side peak in p+p collisions is absent in central d+Au collisions, in agreement with the behavior predicted in [10]. In Fig. 8a, these data are compared with the rcBK calculations of [7]. As mentioned before, the complete near-side peak is not computed, as Eq. (12) does not apply around $\Delta\phi = 0$.

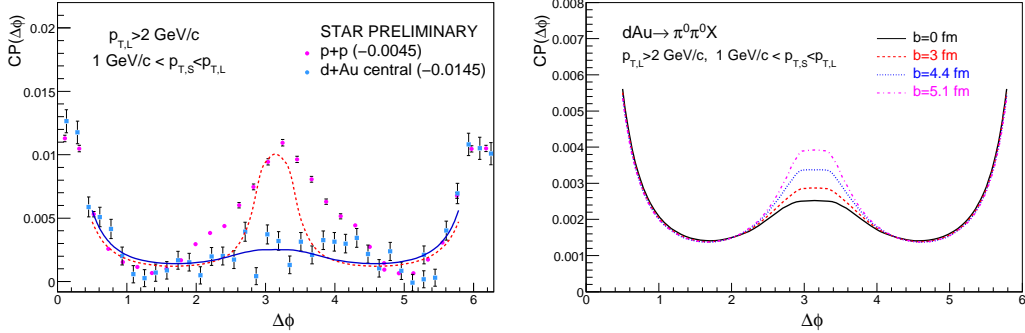


Figure 8: The coincidence probability as a function of $\Delta\phi$. Left: for p+p and central d+Au collisions, preliminary data are compared with CGC predictions; the away-side peak in p+p is qualitatively described by the CGC calculation while its disappearance in central d+Au is quantitatively consistent with the prediction. Right: CGC predictions for different centralities of the d+Au collision; the near-side peak is independent of the centrality, while the away-side peak reappears as collisions are more and more peripheral.

We see that the disappearance of the away-side peak in central d+Au collisions, compared to p+p collisions, is quantitatively consistent with the CGC calculations. The latter are only robust for the d+Au case, but the extrapolation to the p+p case is displayed in order to show that it is qualitatively consistent with the presence of the away-side peak in p+p, and also with the fact that the near-side peak is identical in the two cases, and is not sensitive to saturation physics. Note that since uncorrelated background has not been extracted from the data, the overall normalization of the data points has been adjusted by subtracting a constant shift, as indicated on the figure.

To deal with the centrality dependence, we have identified the centrality averaged initial saturation scale \bar{Q}_{s0}^2 , extracted from minimum-bias single-inclusive hadron production data, with the value of Q_{s0}^2 at $b = 5.47$ fm, and used the Woods-Saxon distribution $T_A(b)$ to calculate the saturation scale at other centralities:

$$Q_{s0}^2(b) = \frac{\bar{Q}_{s0}^2 T_A(b)}{T_A(5.47 \text{ fm})}, \quad \bar{Q}_{s0}^2 = 0.4 \text{ GeV}^2. \quad (15)$$

The value used in Fig. 8a in the central d+Au case is $Q_{s0}^2(0) \simeq 0.6 \text{ GeV}^2$ at $x_0 = 0.02$. The corresponding saturation scale felt by gluons is about 1.2 GeV^2 and of course it gets bigger with decreasing x .

In Fig. 8b, we show the centrality dependence of the coincidence probability. Although it is difficult to trust our formalism all the way to peripheral collisions, we predict that the near-side peak does not change with centrality, and that the away-side peak reappears for less central collisions. This is consistent with the fact that peripheral d+Au collisions are p+p collisions. The fact that the away-side peak disappears from peripheral to central collisions shows that indeed this effect is correlated with the nuclear density.

Moreover dihadron correlations at mid-rapidity, which are sensitive to larger values of x_A , feature an away-side peak whatever the centrality. The fact that for central collisions the away-side peak disappears from central to forward rapidities also indicates that the effect is correlated with the nuclear gluon density. In a similar way, we predict that for higher transverse momenta, the away-side peak will reappear.

We are not aware of any descriptions of this phenomena that does not invoke saturation effects. We note that apart from our CGC calculation, a successful description based on the KLN saturation model was also recently proposed [38]. There, although different assumptions are used, the existence of the saturation scale is the crucial ingredient to successfully reproduce the data. While more differential measurements of the coincidence probability, as a function of transverse momentum or rapidity, will provide further quantitative tests of our CGC predictions, the piece of evidence we have discussed in this work strongly indicates that we have observed manifestations of the saturation regime of QCD at RHIC.

4. Predictions for the LHC

The huge leap forward in collision energy reached at the LHC allows for an exploration of small- x effects already at mid-rapidity. There, both the target and projectile are probed at small values of x , and energy loss effects associated to large- x_F effects are expected to be small. In Fig. 9 we present our CGC predictions for the nuclear modification factor for negative charged hadrons in p+Pb collisions at two LHC energies. Our curves correspond to rapidities $y = 2$ and larger. Technical difficulties related to the intrinsic asymmetry of the hybrid formalism used for particle production prevent us from calculating the ratios at mid-rapidity. However, the smooth rapidity dependence suggests that a large suppression ~ 0.6 is also expected at mid-rapidity in the LHC. It should be taken into account that the normalization taken to produce the curves in Fig. 9 was $N_{coll} = 3.6$.

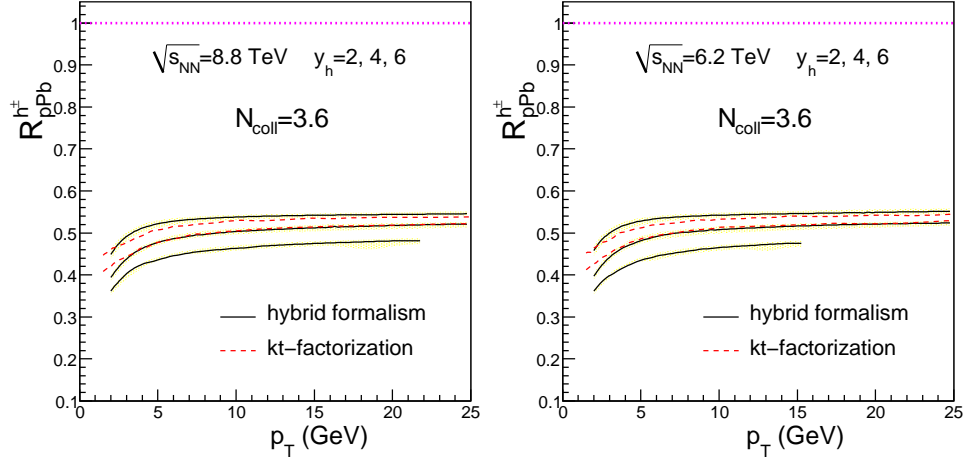


Figure 9: CGC predictions for the nuclear modification factor in p+Pb collisions at two LHC energies and rapidities $y = 2, 4$ and 6 .

We also compare the $y = 2$ and 4 curves with predictions obtained with the k_T -factorization formalism, in order to check the validity of that approach, and especially to test up to what value of y it can be used. The k_T -factorization formula (see [6]) is valid when the dominant contributions to the cross section come from small values of x , for both the projectile ($x_p \ll 1$) and the target ($x_A \ll 1$). For instance, it only includes gluonic degrees of freedom. This approach is clearly insufficient at very forward rapidities or large p_\perp , where valence quarks of the projectile are important ($x_p \rightarrow 1$). However, as can be seen in Fig. 9, both formalisms give comparable results, as the lines from k_T -factorization overlap with the uncertainty bands spanned by the results from the hybrid formalism. This seems to identify a kinematical window where both approximations are valid.

References

- [1] F. Gelis, E. Iancu, J. Jalilian-Marian, R. Venugopalan, The Color Glass Condensate (2010).
- [2] H. Weigert, Evolution at small x : The color glass condensate, Prog. Part. Nucl. Phys. 55 (2005) 461–565.

- [3] I. Arsene, et al., On the evolution of the nuclear modification factors with rapidity and centrality in d + Au collisions at $s(\text{NN})^{1/2} = 200\text{-GeV}$, Phys. Rev. Lett. 93 (2004) 242303.
- [4] J. Adams, et al., Forward neutral pion production in p+p and d+Au collisions at $s(\text{NN})^{1/2} = 200\text{-GeV}$, Phys. Rev. Lett. 97 (2006) 152302.
- [5] E. Braidot, f. t. S. collaboration, Suppression of Forward Pion Correlations in d+Au Interactions at STAR (2010).
- [6] J. L. Albacete, C. Marquet, Single Inclusive Hadron Production at RHIC and the LHC from the Color Glass Condensate, Phys. Lett. B687 (2010) 174–179.
- [7] J. L. Albacete, C. Marquet, Azimuthal correlations of forward di-hadrons in d+Au collisions at RHIC in the Color Glass Condensate (2010).
- [8] D. Kharzeev, Y. V. Kovchegov, K. Tuchin, Cronin effect and high-p(t) suppression in p a collisions, Phys. Rev. D68 (2003) 094013.
- [9] J. L. Albacete, N. Armesto, A. Kovner, C. A. Salgado, U. A. Wiedemann, Energy dependence of the Cronin effect from non-linear QCD evolution, Phys. Rev. Lett. 92 (2004) 082001.
- [10] C. Marquet, Forward inclusive dijet production and azimuthal correlations in pA collisions, Nucl. Phys. A796 (2007) 41–60.
- [11] K. J. Eskola, H. Paukkunen, C. A. Salgado, EPS09 - a New Generation of NLO and LO Nuclear Parton Distribution Functions, JHEP 04 (2009) 065.
- [12] A. Accardi, M. Gyulassy, Cronin effect vs. geometrical shadowing in d + Au collisions at RHIC, Phys. Lett. B586 (2004) 244–253.
- [13] D. Kharzeev, Y. V. Kovchegov, K. Tuchin, Nuclear modification factor in d + Au collisions: Onset of suppression in the color glass condensate, Phys. Lett. B599 (2004) 23–31.
- [14] J.-w. Qiu, I. Vitev, Coherent QCD multiple scattering in proton nucleus collisions, Phys. Lett. B632 (2006) 507–511.

- [15] D. Kharzeev, E. Levin, L. McLerran, Jet azimuthal correlations and parton saturation in the color glass condensate, Nucl. Phys. A748 (2005) 627–640.
- [16] S. S. Adler, et al., Azimuthal angle correlations for rapidity separated hadron pairs in d + Au collisions at $\sqrt{s(NN)}^{1/2} = 200$ -GeV, Phys. Rev. Lett. 96 (2006) 222301.
- [17] B. Meredith, Probing High Parton Densities at Low- x in d+Au Collisions at PHENIX Using the New Forward and Backward Muon Piston Calorimeters, Nucl. Phys. A830 (2009) 595c–598c.
- [18] I. Balitsky, Operator expansion for high-energy scattering, Nucl. Phys. B463 (1996) 99–160.
- [19] Y. V. Kovchegov, Small- x F_2 structure function of a nucleus including multiple pomeron exchanges, Phys. Rev. D60 (1999) 034008.
- [20] I. I. Balitsky, Quark Contribution to the Small- x Evolution of Color Dipole, Phys. Rev. D 75 (2007) 014001.
- [21] Y. Kovchegov, H. Weigert, Triumvirate of Running Couplings in Small- x Evolution, Nucl. Phys. A 784 (2007) 188–226.
- [22] J. L. Albacete, N. Armesto, J. G. Milhano, C. A. Salgado, Non-linear QCD meets data: A global analysis of lepton- proton scattering with running coupling BK evolution, Phys. Rev. D80 (2009) 034031.
- [23] J. L. Albacete, Particle multiplicities in Lead-Lead collisions at the LHC from non-linear evolution with running coupling, Phys. Rev. Lett. 99 (2007) 262301.
- [24] J. L. Albacete, Y. V. Kovchegov, Solving high energy evolution equation including running coupling corrections, Phys. Rev. D75 (2007) 125021.
- [25] A. Dumitru, A. Hayashigaki, J. Jalilian-Marian, The color glass condensate and hadron production in the forward region, Nucl. Phys. A765 (2006) 464–482.
- [26] A. Kovner, U. A. Wiedemann, Eikonal evolution and gluon radiation, Phys. Rev. D64 (2001) 114002.

- [27] Y. V. Kovchegov, K. Tuchin, Inclusive gluon production in DIS at high parton density, *Phys. Rev. D* **65** (2002) 074026.
- [28] C. Marquet, A QCD dipole formalism for forward-gluon production, *Nucl. Phys. B* **705** (2005) 319–338.
- [29] J. Pumplin, et al., New generation of parton distributions with uncertainties from global QCD analysis, *JHEP* **07** (2002) 012.
- [30] D. de Florian, R. Sassot, M. Stratmann, Global analysis of fragmentation functions for pions and kaons and their uncertainties, *Phys. Rev. D* **75** (2007) 114010.
- [31] D. de Florian, R. Sassot, M. Stratmann, Global analysis of fragmentation functions for protons and charged hadrons, *Phys. Rev. D* **76** (2007) 074033.
- [32] B. Z. Kopeliovich, J. Nemchik, I. K. Potashnikova, M. B. Johnson, I. Schmidt, Breakdown of QCD factorization at large Feynman x , *Phys. Rev. C* **72** (2005) 054606.
- [33] L. Frankfurt, M. Strikman, Energy losses in the black disc regime and correlation effects in the STAR forward pion production in d Au collisions, *Phys. Lett. B* **645** (2007) 412–421.
- [34] B. A. Kniehl, G. Kramer, B. Potter, Fragmentation functions for pions, kaons, and protons at next-to-leading order, *Nucl. Phys. B* **582** (2000) 514–536.
- [35] J. Jalilian-Marian, Y. V. Kovchegov, Inclusive two-gluon and valence quark-gluon production in DIS and p A, *Phys. Rev. D* **70** (2004) 114017.
- [36] N. N. Nikolaev, W. Schafer, B. G. Zakharov, V. R. Zoller, Nonlinear $k(T)$ -factorization for quark-gluon dijet production off nuclei, *Phys. Rev. D* **72** (2005) 034033.
- [37] R. Baier, A. Kovner, M. Nardi, U. A. Wiedemann, Particle correlations in saturated QCD matter, *Phys. Rev. D* **72** (2005) 094013.
- [38] K. Tuchin, Rapidity and centrality dependence of azimuthal correlations in Deuteron-Gold collisions at RHIC, *Nucl. Phys. A* **846** (2010) 83–94.